Blur-Invariant Deep Learning for Blind-Deblurring (Supplementary Material)

T M Nimisha
ee13d037@ee.iitm.ac.in

Akash Kumar Singh
ee12b072@ee.iitm.ac.in

A N Rajagopalan
raju@ee.iitm.ac.in

Indian Institute of Technology, Madras, India

We provide additional quantitative and qualitative comparisons on two more publicly available datasets, Köhler et al. [2] and Lai et al. [3] respectively, in this supplementary material to demonstrate the efficacy of our proposed network. We also provide an analysis on the deblurring efficiency and generalizability of our network when compared to a network learned for a single blur kernel. Along with this, we also perform qualitative and quantitative study on the blur kernels. We use least squares to estimate the blur kernel from blur/deblurred pair generated from our network and use a kernel similarity metric to quantify the performance.

S1. Qualitative Comparisons

Figs. S1 - S8 show results of our network along with the outputs obtained from prior-based state-of-the-art conventional methods [4, 9, 11, 8, 5] on randomly chosen images from Lai et al. [3] dataset. The dataset consists of both synthetic and real images collected from various conventional prior works on deblurring. Comparative results are directly taken from [3] and hence it is reasonable to assume that the results for competing methods correspond to their fine-tuned parameters and priors. Figs. S1 - S3 are synthetic examples from this dataset generated using non-uniform camera motions and affected with several common degradations. Rest of the examples are real and are taken from [3]. Fig. S9 contains additional visual results on images captured by us as well as real images taken from [3]. From the exhaustive evaluation given in the main paper and in this supplementary material, it is amply evident that our method yields output that is visually comparable or even better than methods that painstakingly employ different priors on the underlying clean image and kernel for deblurring.

S2. Quantitative Analysis

We also provide quantitative evaluation of our network on the Köhler dataset [2] which is commonly used for evaluating non-uniform deblurring techniques. We have compared against conventional methods [9, 11] and the deep network approach of [7]. The dataset consists of 4 images and 12 non-uniform camera motions totaling to 48 blurred images. The average MSSIM values are provided in Table S1. These numerical values are calculated by using the evaluation code provided in the webpage of [2] and the results for competing methods are obtained by running the code provided by the authors (on their web-page) with default parameter settings for the respective works. Note that the performance of our network is quite comparable with competing methods on this dataset as well. The highlight of our method is that it is quite fast and does not involve any parameter tuning.

	Whyte [9]	**Xu [11]**	**Sun [7]**	**Ours**
MSSIM	0.8405	0.8340	0.7932	0.8102

Table S1. Quantitative comparisons on Köhler dataset [2].

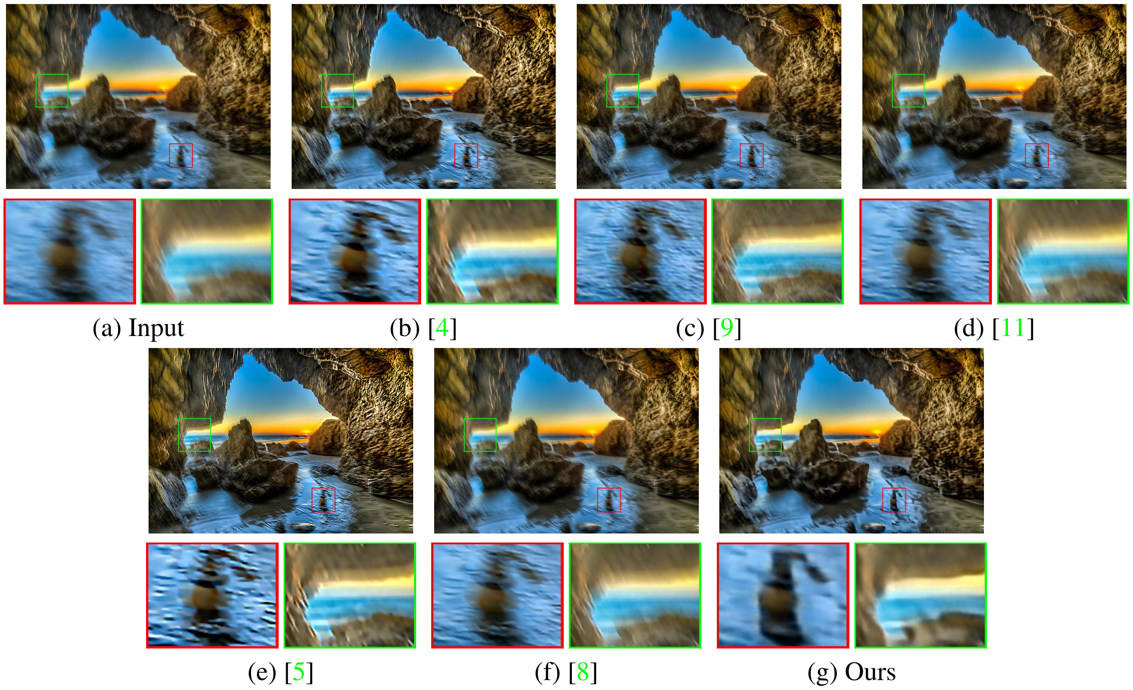

(a) Input (b) [4] (c) [9] (d) [11]

(e) [5] (f) [8] (g) Ours

Figure S1. Synthetic example taken from dataset [3]. (a) Input blurry image. (b-f) Deblurred result corresponding to methods in [4, 9, 11, 5, 8] in order respectively, and (g) is the result obtained by our network. Zoomed-in patches are shown below each of the corresponding result for better viewing.

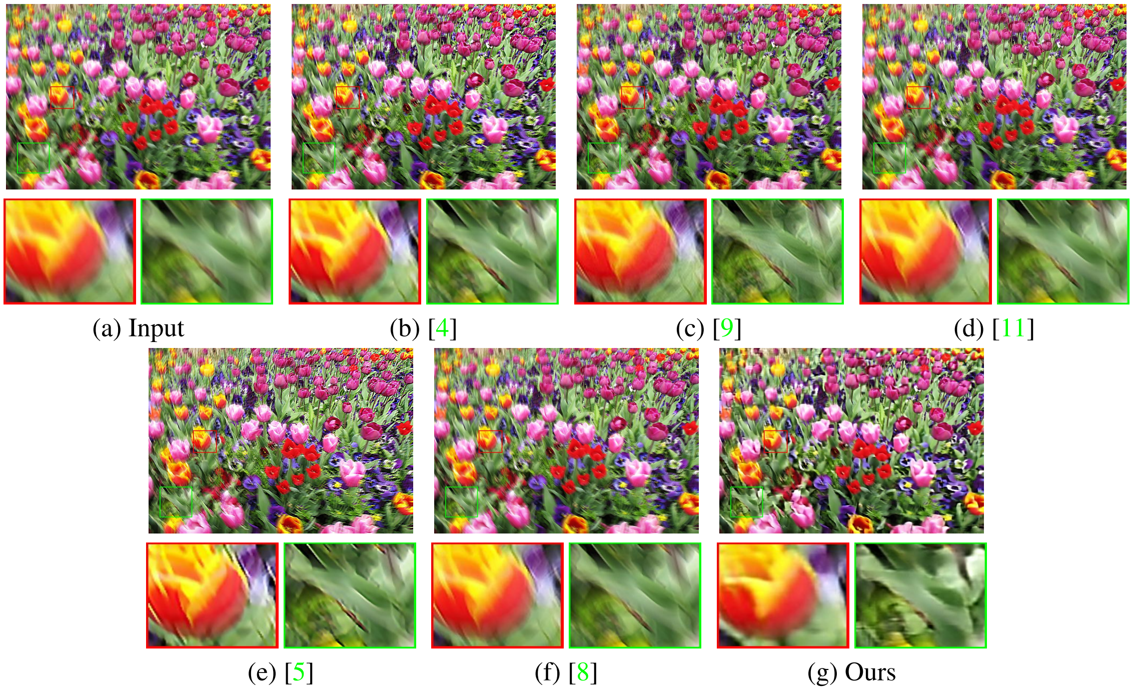

(a) Input (b) [4] (c) [9] (d) [11]

(e) [5] (f) [8] (g) Ours

Figure S2. Another synthetic example from [3] dataset. (a) Input blurry image. (b-f) Deblurred result corresponding to methods in [4, 9, 11, 5, 8] in order respectively, and (g) is the result obtained by our network. The zoomed in patch of leaves is much clear in our result.

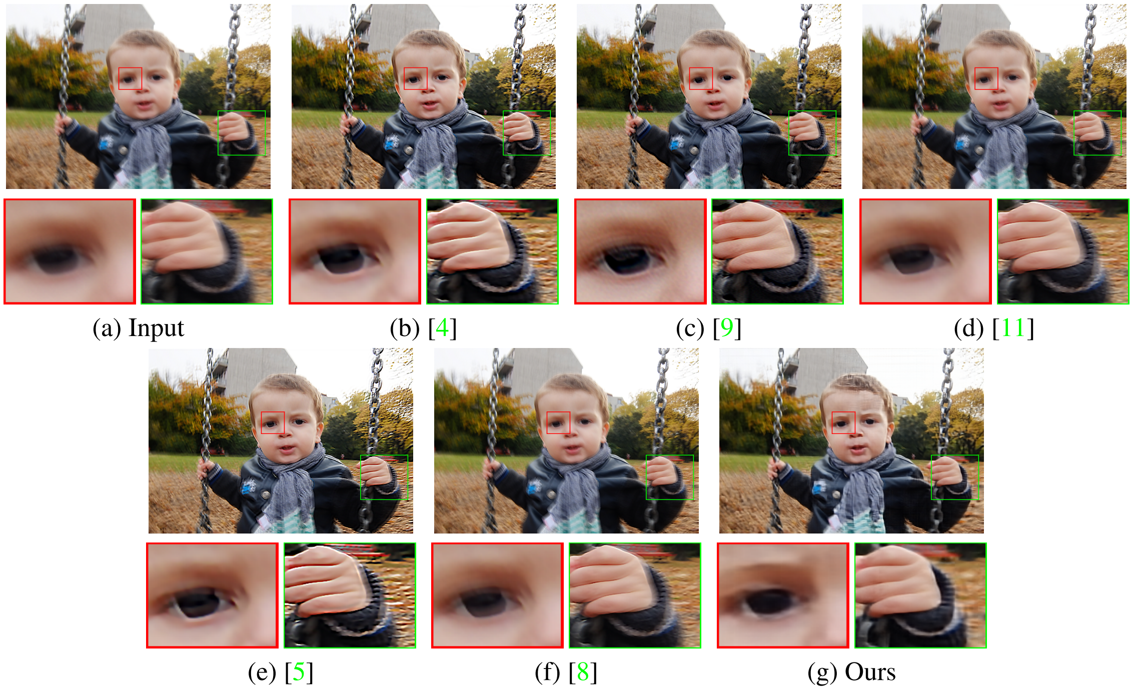
(a) Input (b) [4] (c) [9] (d) [11]

(e) [5] (f) [8] (g) Ours

Figure S3. Synthetic example taken from dataset [3]. (a) Input blurry image. (b-f) Deblurred result corresponding to methods in [4, 9, 11, 5, 8] in order respectively, and (g) is the result obtained by our network. Here the kid's eye and hand look more clear in our result.

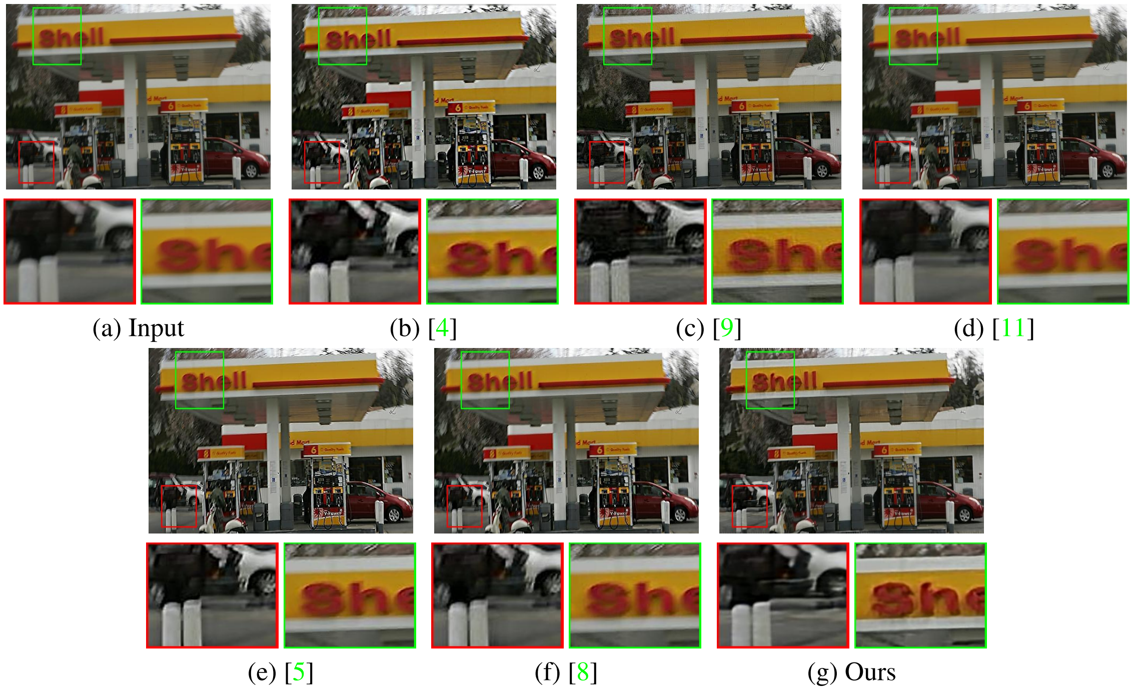
(a) Input (b) [4] (c) [9] (d) [11]

(e) [5] (f) [8] (g) Ours

Figure S4. Visual comparison with conventional methods on real example. Our method generates output that are at par or better than the state-of-the-art methods.

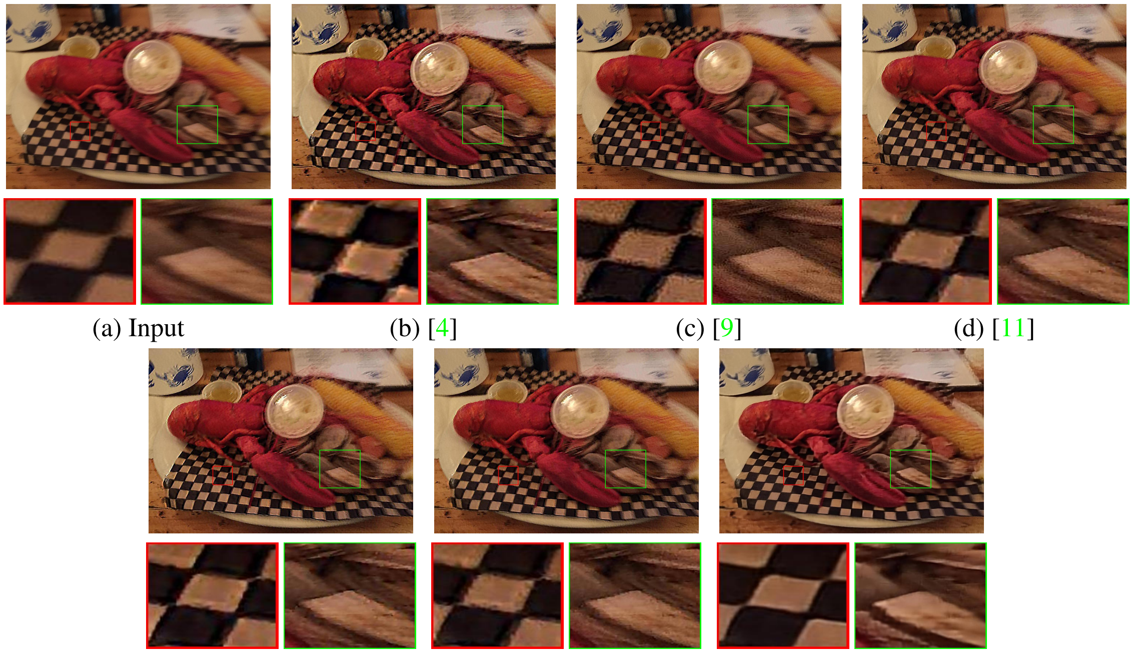

(a) Input (b) [4] (c) [9] (d) [11]

(e) [5] (f) [8] (g) Ours

Figure S5.

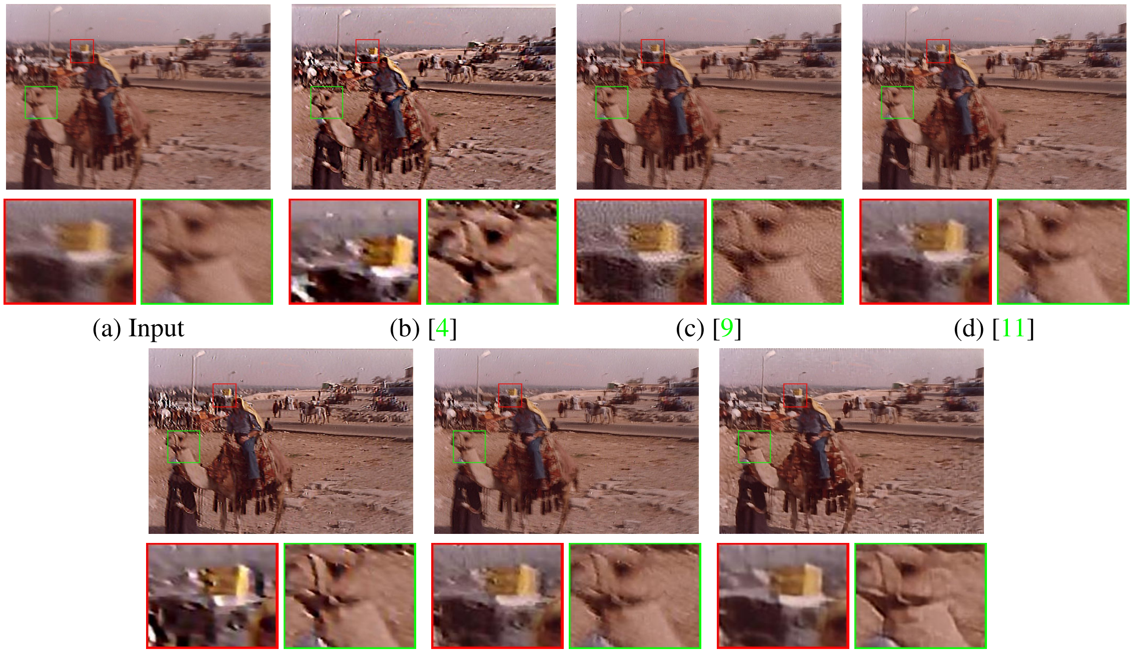

(a) Input (b) [4] (c) [9] (d) [11]

(e) [5] (f) [8] (g) Ours

Figure S6.

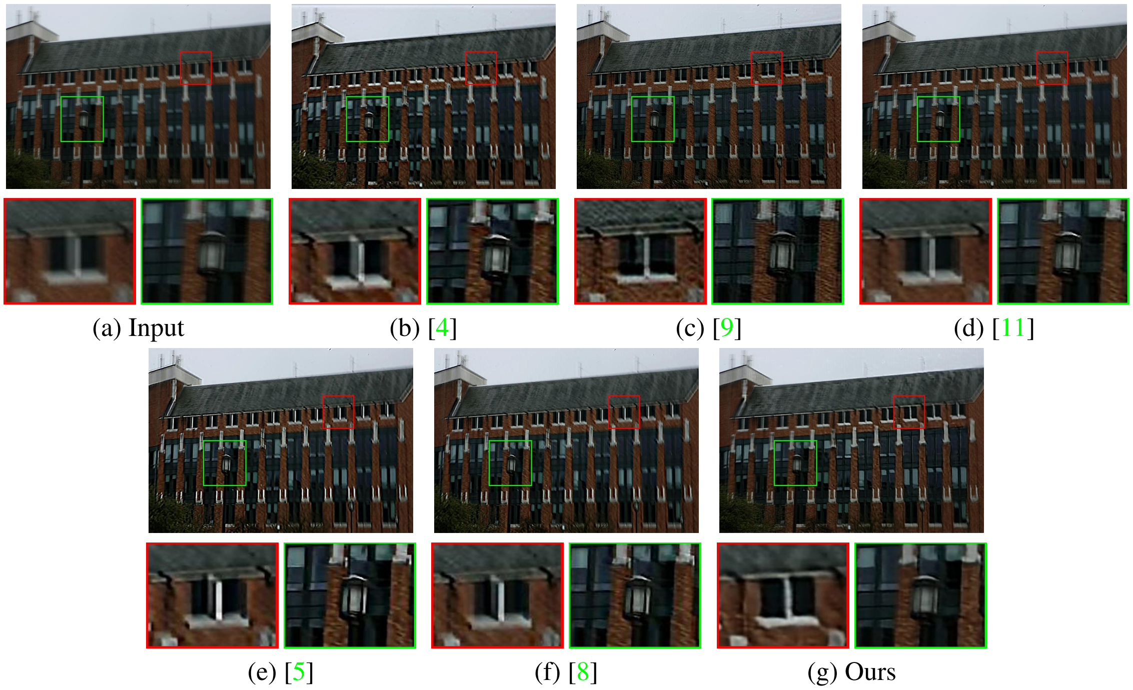

(a) Input (b) [4] (c) [9] (d) [11]

(e) [5] (f) [8] (g) Ours

Figure S7.

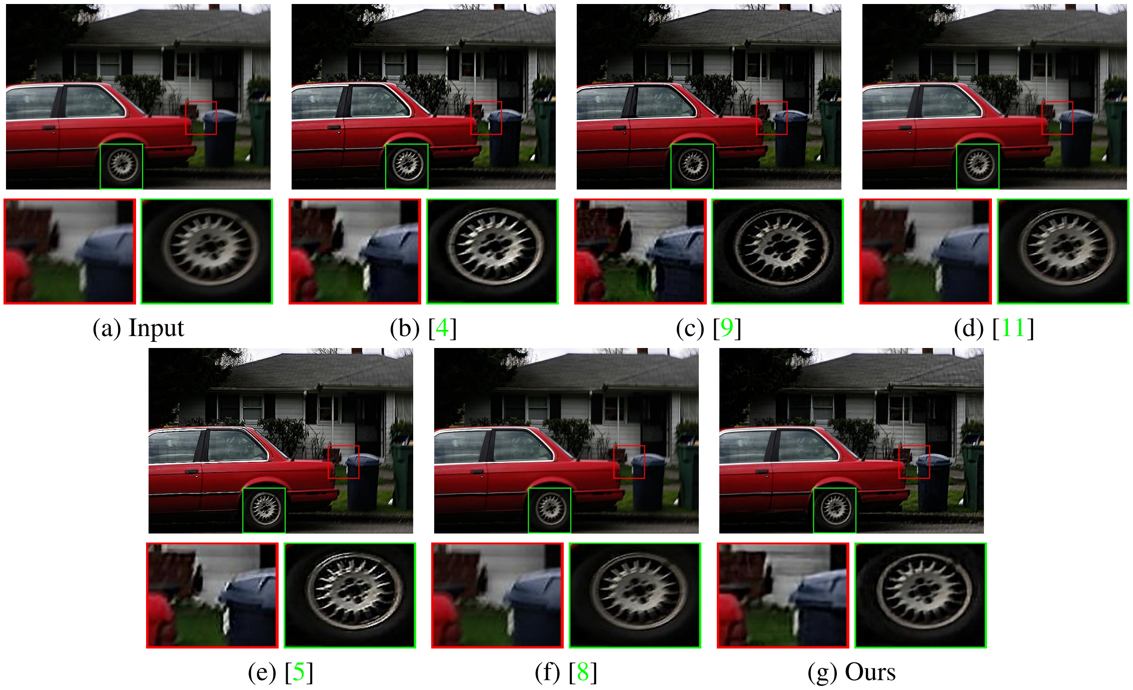

(a) Input (b) [4] (c) [9] (d) [11]

(e) [5] (f) [8] (g) Ours

Figure S8.

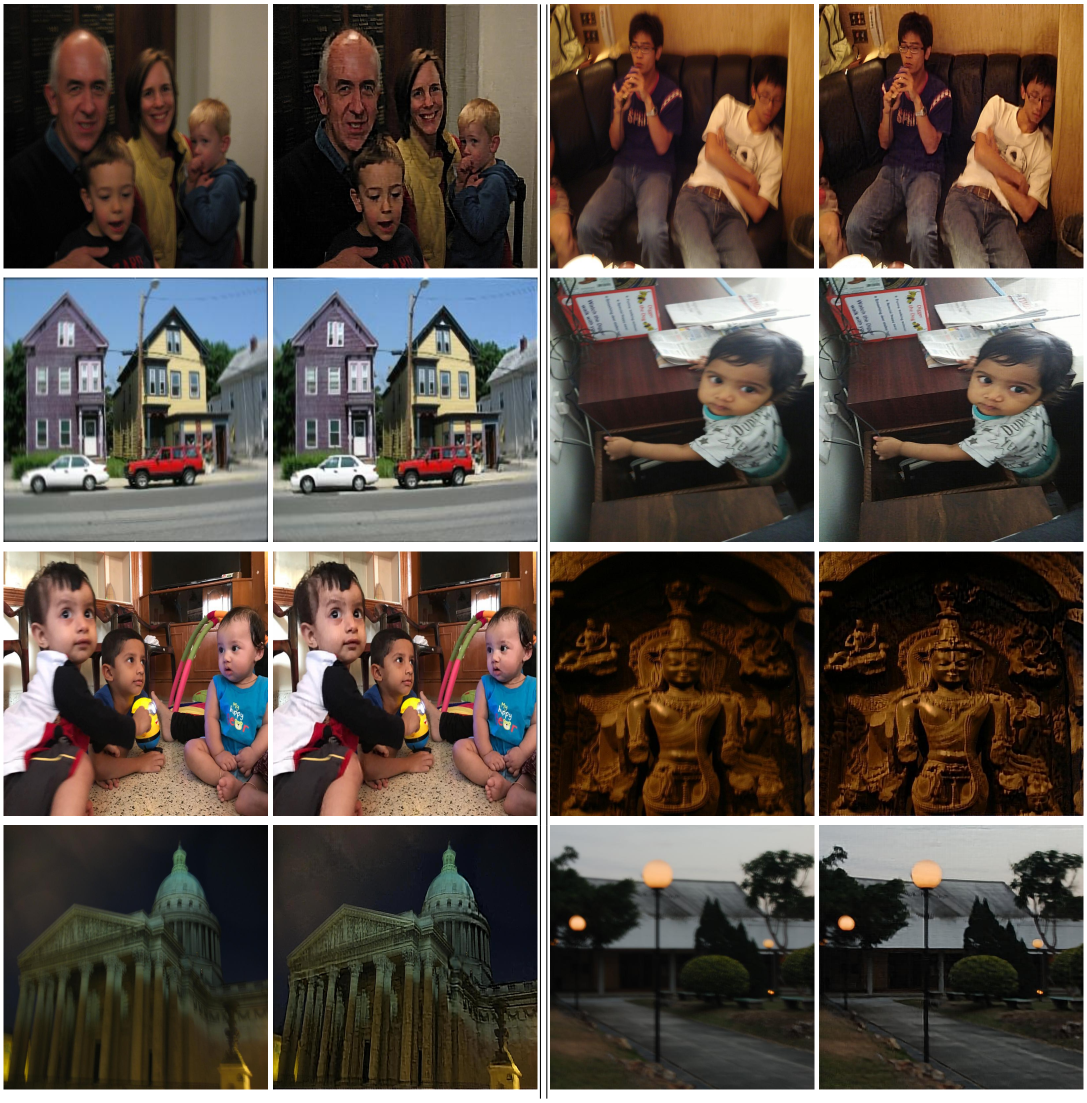

Figure S9. Additional qualitative results for images picked randomly from [3], and captured by ourself. Input in the left side and corresponding output in the right.

S3. Generalizability and Deblurring Quality Trade-off

We have observed that when the network was learned for a single kernel (eg. parameterized by length and angle $\{l, \theta\} = \{6, 45\}$) (NW1), the deblurred result obtained was much sharper and clear for that specific blur but performs poorly on other kernels. The generalization capability and quality of deblurring (PSNR dB) obtained on test dataset (consisting of images with blur equal to $\{l, \theta\} = \{6, 45\}$ as well as on some images from dataset [8] with arbitrary blur) using NW1 and our generalized network is given below.

	Inputs with blur $\{l, \theta\} = \{6, 45\}$	**Dataset [8]**
NW1	29.86	24.29
Our network	28.67	29.48

Table S2. Generalization capability and deblurring efficiency of NW1 and our proposed network.

From Table S2 it can be seen that our network generalizes better. But NW1 will be best suited for the blur it is trained on.

S4. Kernel Estimation

To demonstrate the performance of our deblurring, we estimated the blur kernels(using least squares with TV regularization on motion) from the blur/deblur pairs for dataset [4] and quantified performance using the (average) kernel similarity measure (S) proposed in Hu et al.[1]

Method	**Pan [6]**	**Xu & Jia [10]**	**Xu [11]**	Ours
S	0.8024	0.8002	0.8053	0.8022

Table S3. Average kernel similarity measure estimated for kernels obtained on the dataset [4].

The quantitative measure in Table S3 shows that the kernel estimated with blur/deblur pair from our method is reasonable and comparable to others. Qualitative result of the estimated kernel using our deblurred output is shown in Fig S10 with Fig S10(c) being the ground truth kernels and Fig S10(e) the estimated kernels, respectively.

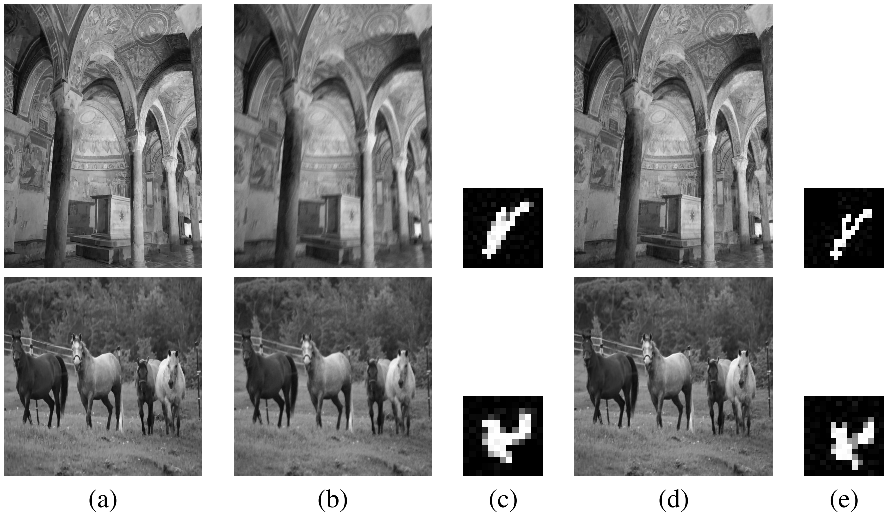

Figure S10. Kernel Estimation. (a) Latent frame. (b) Blurred image synthesized from (a) using the kernel in (c). (d-e) Deblurred output from our network and corresponding blur kernel estimated using (b)/(d) pair is provided in (e).

References

[1] Z. Hu and M.-H. Yang. Good regions to deblur. *Computer Vision–ECCV 2012*, pages 59–72, 2012. 7

[2] R. Köhler, M. Hirsch, B. Mohler, B. Schölkopf, and S. Harmeling. Recording and playback of camera shake: Benchmarking blind deconvolution with a real-world database. In *European Conference on Computer Vision*, pages 27–40. Springer, 2012. 1

[3] W.-S. Lai, J.-B. Huang, Z. Hu, N. Ahuja, and M.-H. Yang. A comparative study for single image blind deblurring. In *Proceedings of the IEEE Conference on Computer Vision and Pattern Recognition*, pages 1701–1709, 2016. 1, 2, 3, 6

[4] A. Levin, Y. Weiss, F. Durand, and W. T. Freeman. Understanding blind deconvolution algorithms. *TPAMI*, 33(12):2354–2367, 2011. 1, 2, 3, 4, 5, 7

[5] J. Pan, Z. Hu, Z. Su, and M.-H. Yang. Deblurring text images via l0-regularized intensity and gradient prior. In *Proceedings of the IEEE Conference on Computer Vision and Pattern Recognition*, pages 2901–2908, 2014. 1, 2, 3, 4, 5

[6] J. Pan, D. Sun, H. Pfister, and M.-H. Yang. Blind image deblurring using dark channel prior. In *CVPR*, pages 1628–1636, 2016. 7

[7] J. Sun, W. Cao, Z. Xu, and J. Ponce. Learning a convolutional neural network for non-uniform motion blur removal. In *CVPR*, pages 769–777. IEEE, 2015. 1

[8] L. Sun, S. Cho, J. Wang, and J. Hays. Edge-based blur kernel estimation using patch priors. In *ICCP*, pages 1–8. IEEE, 2013. 1, 2, 3, 4, 5, 7

[9] O. Whyte, J. Sivic, A. Zisserman, and J. Ponce. Non-uniform deblurring for shaken images. *IJCV*, 98(2):168–186, 2012. 1, 2, 3, 4, 5

[10] L. Xu and J. Jia. Two-phase kernel estimation for robust motion deblurring. In *ECCV*, pages 157–170. Springer, 2010. 7

[11] L. Xu, S. Zheng, and J. Jia. Unnatural l0 sparse representation for natural image deblurring. In *CVPR*, pages 1107–1114, 2013. 1, 2, 3, 4, 5, 7